Journal of Medicinal Chemistry

Article

pubs.acs.org/jmc

Synthesis of New 7-Oxycoumarin Derivatives As Potent and Selective Monoamine Oxidase A Inhibitors

Omaima M. Abdelhafez,*[,†] Kamelia M. Amin,[‡] Hamed I. Ali,[§] Mohamed M. Abdalla,[∥] and Rasha Z. Batran[†]

[†]Chemistry of Natural Products Department, National Research Center, Dokki, Egypt

[‡]Pharmaceutical Chemistry Department, Faculty of Pharmacy, Cairo University, Egypt

[§]Pharmaceutical Chemistry Department, Faculty of Pharmacy, Helwan University, Egypt

[∥]Research Unit, Mapco Pharmaceutical Industries Balteim, Egypt

Supporting Information

ABSTRACT: New series of 4-methyl and 3,4-dimethyl-7-oxycoumarin derivatives (oxadiazoles, thiadiazoles, triazoles, and thiazolidinones) were designed, synthesized, and evaluated for their monoamine oxidase (MAO) A and B inhibiting effect. All the synthesized compounds showed in vitro high affinity and selectivity toward MAO-A isoenzyme, compared to clorgyline and moclobemide, with K_i values on the picomolar range. Moreover, most of the tested compounds displayed MAO inhibitory effect when tested in vivo. The docking experiments carried out on MAO-A and MAO-B structures proved new information about the enzyme−inhibitor interaction and the potential therapeutic application of 7-oxycoumarin scaffold.

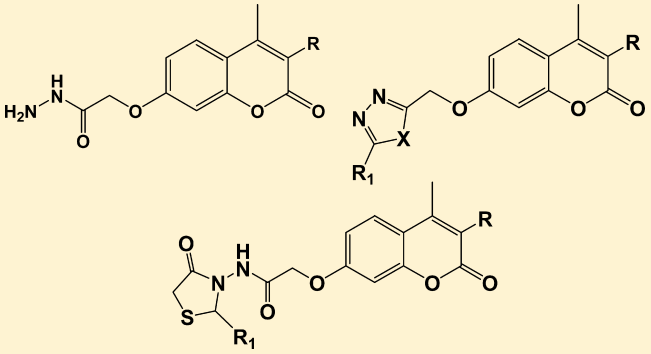

INTRODUCTION

Monoamine oxidases (MAOs) are FAD depending enzymes responsible for the regulation and metabolism of major monoamine neurotransmitters (5-hydroxytryptamine (5-HT), norepinephrine (NE), and dopamine (DA)), modulating their concentrations in the brain and peripheral tissues.[1,2] They are also involved in the biodegradation of exogenous amines such as 1-methyl-4-phenyl-1,2,3,6-tetrahydropyridine (MPTP) into 1-methyl-4-phenyl pyridinium (MPP^+), a Parkinson producing neurotoxin.[3−5] The MAO enzyme exists in two forms, namely MAO-A and MAO-B, distinguishable by their molecular cloning, substrate and inhibitor selectivity, and tissue distribution.[6−9] MAO-A preferentially oxidizes serotonin and is irreversibly inhibited by low concentrations of clorgyline,[7] while that of the B isoform preferentially oxidizes β-phenylethylamine (PEA) and benzylamine and it is irreversibly inactivated by low concentrations of L-deprenyl.[10] Dopamine, tyramine, and tryptamine are common substrates for both MAOs. In fact, human MAO-A inhibitors are antidepressants and antianxiety agents,[11] while human MAO-B inhibitors are used alone or in combination with other drugs in the therapy of Alzheimer's and Parkinson's diseases.[12,13]

Among several MAO inhibitors, some (2*H*)-1- benzopyran-2-one derivatives (coumarins) were screened for their good MAO inhibitory activities.[14−16] At the same time, a great deal of literature data on the importance of substitution of 7-oxycoumarin nucleus with a methyl group at position 3 and/or 4 considers it crucial for modulating MAO-B inhibitory activity and A/B selectivity.[17,18] So far, the aforementioned studies, encouraged us to assay a large array of 4-methyl (and 3,4-dimethyl)-7-oxycoumarins incorporated with different bioactive moieties known to have MAO inhibition activity as oxadiazoles,[19,20] thiadiazoles,[21,22] triazoles,[23] and thiazolidinones[23] in order to evaluate their anti-MAO effect in vitro and in vivo. Finally, docking experiments were carried out on MAO-A and MAO-B crystallographic structures on the basis of the significant structural information currently available on MAOs[24−26] in order to analyze the structural requirements for MAO activity and selectivity.

CHEMISTRY

The 7-oxycoumarin derivatives (**1a,b**), (**2a−d**), (**3a−h**), (**4a,b**), (**5a,b**), (**6a,b**), (**7a,b**), (**8a−d**), (**9a−d**), and (**10a,b**) were efficiently synthesized according to the protocols outlined in Schemes 1−3. The general reaction conditions and the compounds characterization are described in the Experimental Section.

The key intermediates, 5-mercapto-1,3,4-oxadiazoles (**2a**,[27] **2b**), were prepared by refluxing hydrazides (**1a**,[28] **1b**[29]) with carbon disulfide in alcoholic potassium hydroxide solution while the reaction of the same hydrazides (**1a,b**) with carbon

Received: July 12, 2012
Published: November 15, 2012

disulfide in alcoholic potassium hydroxide at room temperature followed by cyclization with conc H_2SO_4, gave the corresponding 5-mercapto-1,3,4-thiadiazole derivatives (**2c**,[27] **2d**).

In addition, *S*-alkylation of (**2a−d**) with diethylaminoethylchloride hydrochloride and/or morpholinoethylchloride hydrochloride, in refluxing acetone in the presence of potassium carbonate, afforded the target diethylaminoethylthio-1,3,4-oxadiazole compounds (**3a,b**), diethylaminoethylthio-1,3,4-thiadiazoles (**3c,d**), morpholinoethylthio-1,3,4-oxadiazoles (**3e,f**), and morpholinoethylthio-1,3,4-thiadiazole derivatives (**3g,h**), respectively (Scheme 1).

Scheme 1

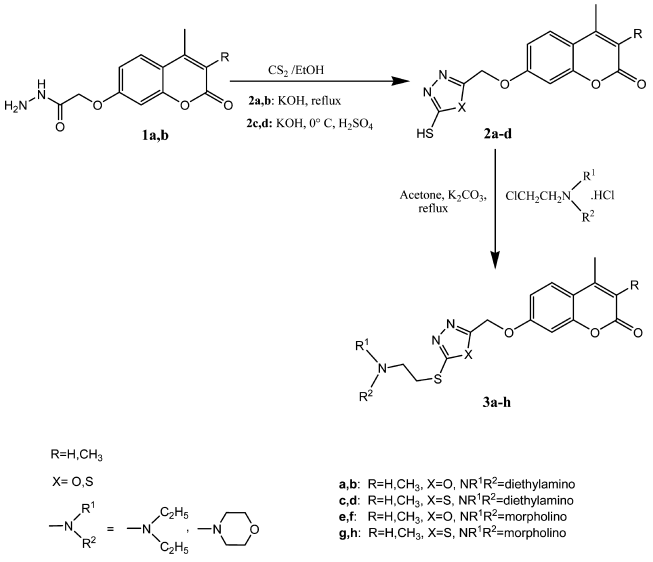

Condensation of the hydrazides (**1a,b**) with 4-chlorophenylisothiocyanate afforded the thiosemicarbazide derivatives (**4a**,[30] **4b**), which were further cyclized with H_2SO_4 to get 4-chlorophenylaminothiadiazoles (**5a**,[30] **5b**) and with chloroacetic acid to afford the corresponding iminothiazolidinone derivatives (**6a,b**). Moreover, refluxing thiosemicarbazides (**4a,b**) with sodium hydroxide yielded the corresponding 5-mercapto-1,2,4-triazoles (**7a**,[30] **7b**), which were reacted with diethylaminoethylchloride hydrochloride and/or morpholinoethylchloride hydrochloride, in acetone in the presence of potassium carbonate, to give the target diethylaminoethyl thio-1,3,4-triazoles (**8a,b**) and morpholinoethylthio-1,3,4-triazole derivatives (**8c,d**), respectively (Scheme 2).

Furthermore, the Schiff's bases (**9a**),[28] (**9b**), (**9c**),[28] and (**9d**) were prepared by the reaction of hydrazides (**1a,b**) with 4-chlorobenzaldehyde and/or 4-chloroacetophenone. Heterocyclization of the aforementioned Schiff's bases (**9a,b**) with mercaptoacetic acid yielded the corresponding thiazolidinone derivatives (**10a,b**) (Scheme 3).

BIOLOGY

The synthesized compounds were tested in vitro for their MAO-A and MAO-B inhibiting activity using clorgyline (A-selective, irreversible), moclobemide (A-selective, reversible), and selegiline (B-selective, irreversible) as reference drugs. Bovine brain mitochondria isolated according to Basford[31] were used as a source of the two MAO isoforms. MAO-A and MAO-B activities were determined by a fluorometric assay, using kynuramine as a substrate, in the presence of their specific inhibitors (L-deprenyl 1 μM for MAO-A and clorgyline 1 μM for MAO-B).[32] The inhibitory activities (K_i) and the A-selectivity (SI) of the tested compounds are depicted in Table 1. All the tested compounds were found to act through a noncompetitive and reversible mode as demonstrated by the fact that dialysis for 24 h at 5 °C against 0.1 M potassium phosphate buffer at pH 7.2 was able to restore 95−100% of the enzyme activity. The substrate did not compete with the inhibitor, accordingly, a decrease of V_{max} was observed, while the K_m value was unchanged.

Moreover, the in vivo inhibiting properties of the synthesized compounds (Table 2) were also elucidated using the in vivo tryptamine seizure potentiation procedure in rats regarding that monoamine oxidase inhibitors like iproniazid enhance the seizures caused by an intravenous infusion of tryptamine hydrochloride in rats.[33,34]

DOCKING STUDIES

Although significant advances in the design of selective MAOIs were achieved in the past two decades, a veritable breakthrough in the field occurred only few years ago with the resolution of the X-ray crystal structure of human MAO-B (hMAO-B)[35] and rat MAO-A (rMAO-A).[36] The high-resolution 3D structure of the hMAO-B in complex with a large number of selective inhibitors, covalently bound to the FAD cofactor,[37] finally paved the way to the structure-based design of new modulators of MAO-B activity. This study was performed using the advanced and widely distributed molecular grid-based docking program Autodock 4.2[38] for docking of flexible ligand within flexible protein. The target MAO-A enzyme (PDB 2Z5X)[25]and MAO-B (PDB 2XFN)[39] proteins were involved.

Here, we investigated the AutoDock binding affinities into MAO-A and MAO-B for the synthesized thirty-two coumarin derivatives, (**1a,b**), (**2a−d**), (**3a−h**), (**4a,b**), (**5a,b**), (**6a,b**), (**7a,b**), (**8a−d**), (**9a−d**), and (**10a,b**). This study was carried out by differential docking of the compounds into the structure of human monoamine oxidase A (PDB 2Z5X)[25] with its 7-methoxy-1-methyl-9*H*-β-carboline (HRM)[25] bound ligand and the human monoamine oxidase B (PDB 2XFN)[39] in complex with 2-(2-benzofuranyl)-2-imidazoline (XCG).[39]

As cited in literature,[40] if the RMSD (root-mean-square deviation) of the best docked conformation of the native ligand is ≤2.0 Å from the experimental one, the used scoring function is successful. Therefore the validation of the docking accuracy was investigated for MAO-A and MAO-B enzymes, to inspect how closely the best docked conformations resemble the bound ligands in the biological methods.[25,39]

Within MAO-A receptor, the docked ligand **1** (HRM) was bound hydrophobically with the key amino acids of MAO-A, and it seemed superimposed on the native ligand within RMSD of 0.28 Å. The obtained success rates of AutoDock were highly excellent,as displayed in Table 3, and shown in Figure 1A. Whereas, the docked ligand **2** (XCG) was bound efficiently into the target macromolecule of MAO-B identically superimposed onto the natively bound ligand within 0.68 Å, as cited in Table 4 and shown in Figure 1B.

RESULTS AND DISCUSSION

Monoamine Oxidase Inhibiting Effect. *In Vitro MAO-A and MAO-B Inhibitory Effect.* Generally, all the synthesized compounds are exceptionally potent and selective MAO-A inhibitors, and they inhibit MAO-A at a subnanomolar

Scheme 2

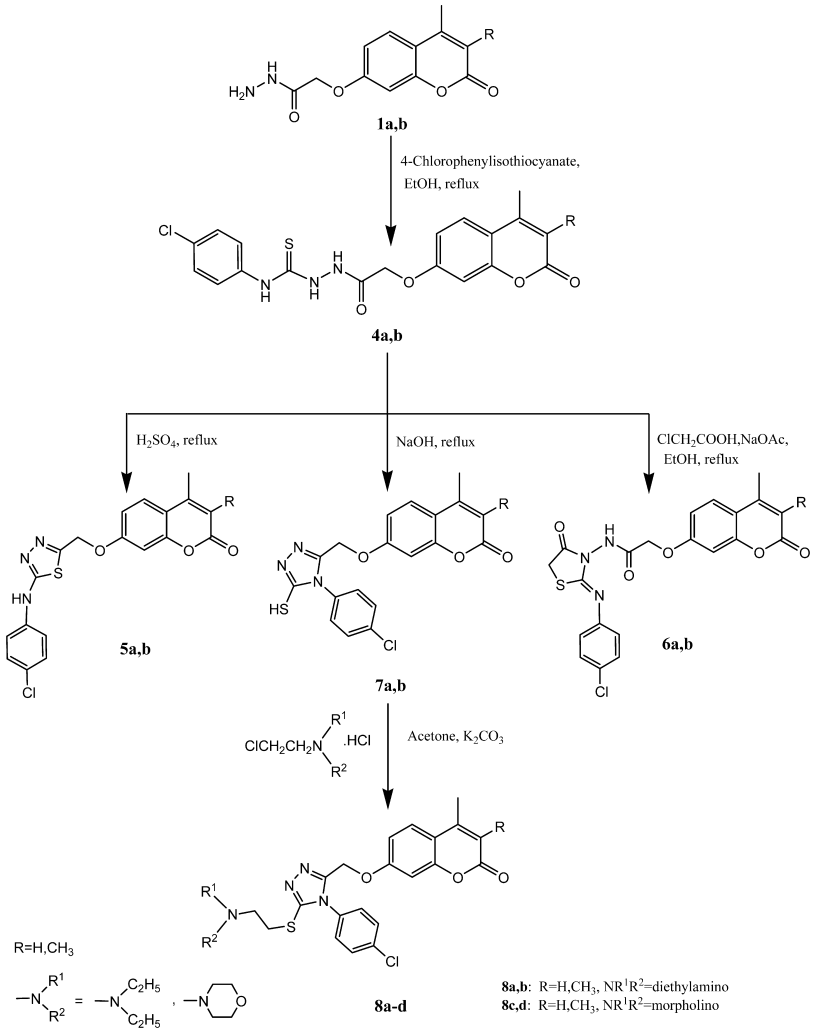

Scheme 3

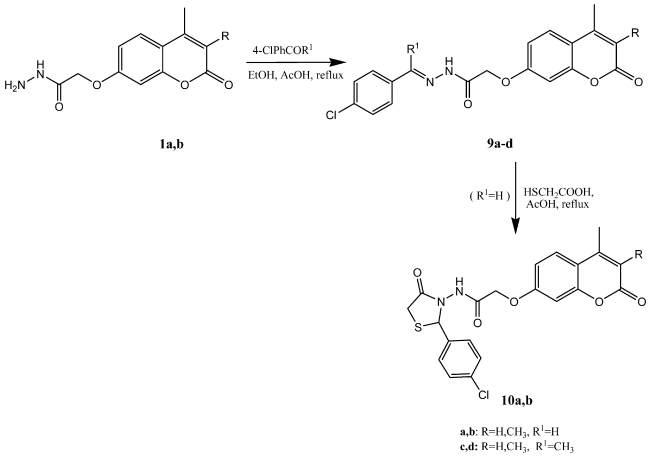

concentration, with K_i values in the picomolar range compared to clorgyline and moclobemide. On the other hand, the synthesized compounds exhibit MAO-B inhibiting activity at a submicromolar concentration, showing an anti-MAO-B effect greater than selegiline (Table 1).

The majority of 3,4-dimethylcoumarinyl-7-oxy derivatives show lower K_i values than the 4-methylcoumarinyl-7-oxy target compounds for both MAO-A and B isoforms. The 3,4-dimethylcoumarin-7-yloxyacetohydrazide (**1b**) is exceptionally the most potent MAO-A and MAO-B inhibitor (K_i (MAO-A) = 5.01 pM, K_i (MAO-B) = 0.484 μM). Demethylation of (**1b**) results in a dramatic drop of MAO-A and MAO-B inhibition (**1a**) (K_i (MAO-A) = 11.20 pM, K_i (MAO-B) = 0.874 μM).

Moreover, *S*-alkylation of the mercaptothiadiazolyl derivative (**2d**) (K_i (MAO-A) = 6.37 pM, K_i (MAO-B) = 0.572 μM) with both diethylaminoethyl (**3d**) and morpholinoethyl (**3h**) moieties increases the in vitro inhibitory effect for both MAO-A and B (K_i (MAO-A) = 5.18 and 5.73 pM, K_i (MAO-B) = 0.496 and 0.535 μM, respectively). Replacement of the thiadiazole ring with its bioisosteric oxadiazole one (**3b**) and (**3f**) results in a decreased inhibitory activity for both MAO-A and MAO-B isoforms (K_i (MAO-A) = 6.58 and 6.39 pM, K_i (MAO-B) = 0.555 and 0.571 μM respectively).

The open chain structures as the thiosemicarbazides (**4a**) and (**4b**) show significant anti-MAO-A and B effects (K_i (MAO-A) = 7.01, 6.51 pM, K_i (MAO-B) = 0.620, 0.561 μM respectively). Additionally, compound (**9b**) proved to be the most potent in vitro tested Schiff's base (K_i (MAO-A) = 5.54 pM, K_i (MAO-B) = 0.522 μM).

On the other hand, the thaizolidinone (**10a**) presents a lower inhibition activity toward MAO-A and B enzymes than its imino derivative (**6a**) (K_i (MAO-A) = 10.9 versus 6.56 pM, K_i

dx.doi.org/10.1021/jm301014y | J. Med. Chem. 2012, 55, 10424−10436

Table 1. MAO-A and B Inhibitory Activities (K_i; pM), and Selectivity (SI) of the Tested Compounds[a]

compd	K_i MAO-A	K_i MAO-B (μM)	SI[b]
1a	11.2 pM	0.874	7.80×10^4
1b	5.01 pM	0.484	9.66×10^4
2a	12.0 pM	0.918	7.65×10^4
2b	6.40 pM	0.570	8.91×10^4
2c	11.0 pM	0.896	8.15×10^4
2d	6.37 pM	0.572	8.98×10^4
3a	6.57 pM	0.556	8.47×10^4
3b	6.58 pM	0.555	8.43×10^4
3c	10.1 pM	0.812	8.01×10^4
3d	5.18 pM	0.496	9.58×10^4
3e	6.53 pM	0.559	8.56×10^4
3f	6.39 pM	0.571	8.93×10^4
3g	9.81 pM	0.792	8.07×10^4
3h	5.73 pM	0.535	9.34×10^4
4a	7.01 pM	0.620	8.84×10^4
4b	6.51 pM	0.561	8.62×10^4
5a	6.38 pM	0.571	8.96×10^4
5b	6.59 pM	0.554	8.41×10^4
6a	6.56 pM	0.557	8.49×10^4
6b	6.35 pM	0.574	9.05×10^4
7a	6.41 pM	0.569	8.89×10^4
7b	6.61 pM	0.553	8.36×10^4
8a	6.45 pM	0.566	8.78×10^4
8b	6.46 pM	0.564	8.73×10^4
8c	6.41 pM	0.569	8.87×10^4
8d	6.42 pM	0.568	8.84×10^4
9a	8.87 pM	0.736	8.30×10^4
9b	5.54 pM	0.522	9.42×10^4
9c	8.02 pM	0.684	8.53×10^4
9d	6.48 pM	0.563	8.69×10^4
10a	10.9 pM	0.853	7.86×10^4
10b	5.93 pM	0.548	9.24×10^4
clorgyline	0.0540 μM	58.0	1.07×10^3
moclobemide	11.5 μM	>100	>87
selegiline	3.80 μM	0.970	2.50×10^{-1}

[a]Data represent mean values (three significant digits) for at least three separate experiments each performed in duplicate. Standard errors were within 2%. [b]SI (selectivity index) = K_i (MAO-B)/K_i (MAO-A) ratio.

Table 2. In Vivo Tryptamine Seizure Potentiation (ED_{50}; nM) by Tested Compounds in Rats

compd	ED_{50} (nM)	compd	ED_{50} (nM)
1a	8.05 ± 0. 12[a]	**5a**	9.67 ± 0.50[a]
1b	9.14 ± 0. 23[a]	**5b**	68.6 ± 5.4
2a	7.85 ± 0. 32[a]	**6a**	48.3 ± 3.4[a]
2b	9.87 ± 0. 65[a]	**6b**	9.26 ± 0.34[a]
2c	7.95 ± 0. 26[a]	**7a**	9.96 ± 0.88[a]
2d	9.55 ± 0. 84[a]	**7b**	81.3 ± 6.6
3a	52.6 ± 3.5[a]	**8a**	106 ± 5
3b	62.7 ± 3.9	**8b**	126 ± 3
3c	8.24 ± 0. 36[a]	**8c**	10.1 ± 0.4[a]
3d	9.05 ± 0. 36[a]	**8d**	26.5 ± 0.5[a]
3e	256 ± 4	**9a**	8.56 ± 0.43[a]
3f	9.78 ± 0. 35[a]	**9b**	74.6 ± 4.8
3g	8.33 ± 0. 36[a]	**9c**	29.6 ± 0.6[a]
3h	75.7 ± 3. 5	**9d**	150 ± 5
4a	41.4 ± 4.6[a]	**10a**	8.16 ± 0.32[a]
4b	196 ± 4	**10b**	76.7 ± 2. 2
iproniazide	64.5 ± 2.2		

[a]Each ED_{50} value is the mean (three significant digits) ± SEM from five experiments. Level of statistical significance: $P < 0.01$ with respect to ED_{50}value of iproniazide as determined by ANOVA/Dunnett's.

(MAO-B) = 0.853 versus 0.557 μM), while substitution of the coumarin ring of (**10a**) with extra 3-methyl group inverses its MAO inhibiting effects (**10b**) (K_i (MAO-A) = 5.93 pM, K_i (MAO-B) = 0.548 μM).

In Vivo Inhibiting Effect. In vivo measurements indicate that both the acetohydrazide compounds (**1a**) and (**1b**) exert a remarkable inhibitory activity (ED_{50} = 8.05, 9.14 nM respectively),being about 7-fold more active than iproniazide (ED_{50} = 64.5 nM).

Furthermore, the mercapto-1,3,4 oxadiazoles (**2a**) and (**2b**) and their thiadiazole bioisosters (**2c**) and (**2d**) elicit significant inhibition potencies (ED_{50} = 7.85, 9.87, 7.95, and 9.55 nM,respectively). In addition, the diethylaminoethyl (**3c**) and (**3d**) and the morpholinoethyl (**3g**) derivatives present comparable potencies to the parent thiadiazolyl compounds (**2c**) and (**2d**) (ED_{50} = 8.24, 9.55, and 8.33 nM, respectively),while a sharp increase in the ED_{50} value is observed for the oxadiazolyl derivatives (**3a**) and (**3e**) (52.6 and 256 nM,respectively) over the parent compound (**2a**).

Moreover, *p*-chlorophenylaminothiadiazolyl- 4-methylcoumarin (**5a**) has much higher anti-MAO effect (ED_{50} = 9.67 nM) compared to the 3,4-dimethylcouamrinyl derivative (**5b**) (ED_{50} = 68.6 nM),which lacks any inhibition effect. In addition, the mercapto-1,2,4-triazolyl-4-methylcoumarin (**7a**) demonstrates the highest in vivo MAO inhibition within the synthesized traizole series (ED_{50} = 9.96 nM).

On the other hand, lower ED_{50} value is observed for the target 4-methylcoumarinyl Schiff's base (**9a**) (ED_{50} = 8.56 nM) than the methyl substituted azomethine derivative (**9c**) (ED_{50} = 29.6 nM), while the 3,4-dimethylcoumarinyl Schiff 's base (**9b**) completely lacks any inhibition effect (ED_{50} = 74.6 nM) .

Finally, the 4-methylcoumarinylthiazolidinone (**10a**) (ED_{50} = 8.16 nM) shows about 6-fold higher in vivo inhibition activity than its imino derivative (**6a**) (ED_{50} = 48.3 nM). Also, it displays about 9-fold higher activity than the 3,4-dimethylcoumarinyl derivative (**10b**) (ED_{50} = 76.7 nM). On the contrary, the 3,4-dimethylcoumarinyliminothiazolidinone derivative (**6b**) (ED_{50} = 9.26 nM) displays much higher potency than the thiazolidinone congener (**10b**) (Table 2).

Molecular Modeling Study. AutoDock binding affinities of the synthesized compounds were evaluated according to many parameters including: the binding free energies (ΔG_b, kcal/mol), inhibition constants (K_i), hydrogen bonding, and RMSD values in comparison to the native cocrystallized ligand. As shown in Table 3, the overall docking results were compared to the crystal structure of the bound native ligand, where the compounds revealing the highest binding affinities, i.e., lowest binding free energies within MAO-A, exhibiting highest numbers of hydrogen bond interactions into the target receptor and of the lowest RMSD values were considered as the best fitted ones. The binding free energies (ΔG_b) were revealed up to −18.55 kcal/mol (K_i, 5.07 fM).

On applying the flexible docking into MAO-A,the promising compounds as drug candidates include compounds: (**9d**), (**7b**), (**4a**), (**2c**), (**2b**), (**7a**), (**1b**), (**1a**), (**3e**), and (**2d**), which reveal binding free energies (ΔGb) being in the range of −16.06 to

dx.doi.org/10.1021/jm301014y | J. Med. Chem. 2012, 55, 10424−10436

Table 3. The Best Results of the Flexible Docking Regarding the Binding Free Energies (ΔG_b) and Inhibition Constants (K_i) of Compounds Docked into MAO-A, the Distances and Angles of Hydrogen Bonds between Compounds and Amino Acids Involved in MAO-A and RMSD from Co-crystallized HRM Native Ligand

			hydrogen bonds between atoms of compounds and amino acids of MAO-A				
compd	ΔG_b[a] (kcal/mol)	K_i[b] (fM)	atom of compd	amino acid	distance (Å)	angle (deg)	RMSD[c] (Å)
1a	−16.74	537.23	2C═O	HO of Tyr444	1.94	142.7	0.90
			2C═O	HN of Asn181	1.91	151.9	
1b	−16.95	378.72	2C═O	HO of Tyr444	2.09	140.5	1.51
			2C═O	HN of Asn181	1.95	166.2	
			terminal NH[a]	O═C of Ala111	2.14	109.3	
			terminal NH[b]	O═C of Ala111	2.27	100.9	
2b	−17.10	293.98	oxadiazole N^3	HN of Val210	2.15	141.4	4.41
			oxadiazole N^4	HN of Val210	2.01	175.0	
2c	−17.10	294.11	2C═O	HO of Tyr444	1.89	153.2	1.05
			2C═O	HN of Asn181	2.00	142.3	
			O (pyrone)	HN of Asn181	2.34	119.4	
			SH (side chain)	O═C of Ala111	1.98	137.6	
2d	−16.06	1680	terminal SH	O═C of Gln215	1.98	115.3	2.15
3e	−16.31	1110	2C═O	HO of Tyr444	2.09	118.0	1.50
			O (pyrone)	HO of Tyr444	1.98	112.7	
4a	−17.75	97.95	2C═O	HN of FAD	1.97	123.7	1.66
			O (pyrone)	HO of Tyr407	2.00	151.2	
4b	−15.49	4400	O (pyrone)	HN of Asn181	2.48	121.0	2.52
			O (pyrone)	HO of Tyr444	2.40	153.5	
			p-NH	HS of Cys323	2.43	121.0	
5a	−15.58	3780	*d*	*d*	*d*	*d*	1.67
5b	−15.82	2540	2C═O	HN of Asn181	1.93	131.0	0.33
			2C═O	HO of Tyr444	2.08	115.6	
			p-NH	HS of Cys323	2.39	123.8	
7a	−16.96	229.51	SH (side chain)	O═C of Gln215	2.18	124.4	1.25
7b	−17.99	64.72	O (pyrone)	HO of Tyr444	2.35	111.3	1.33
8c	−15.36	5530	O (pyrone)	HN of Asn181	2.26	123.9	2.08
			O (morpholin)	HN of Val210	2.38	133.3	
9b	−17.78	92.40	*d*	*d*	*d*	*d*	3.00
9d	−18.55	25.07	2C═O	HN of Asn181	2.25	146.2	2.26
			2C═O	HO of Tyr444	1.88	146.9	
HRM[e]	−15.72	3020	*d*	*d*	*d*	*d*	0.28

[a]Binding free energy. [b]Inhibition constant. [c]Root mean square deviation. [d]No hydrogen bond detected. [e]XCG: 2-(2-benzofuranyl)-2-imidazoline.

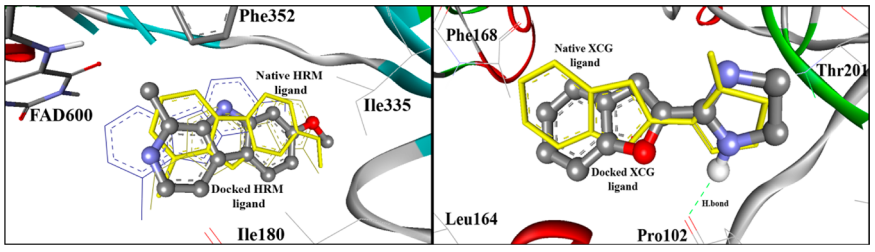

Figure 1. Evaluation of AutoDock 4.2 program by redocking of the native ligands HRM and XCG into MAO-A and MAO-B, as shown in (A) and (B), respectively. Different runs of the docked HRM ligand into MAO-A, all runs (ball and stick and lines, colored by elements), and the docked ligand XCG (ball and sticks, colored by element) into MAO-B, all seem superimposed onto the native cocrystallized ones (yellow sticks) within RMSD 0.28 and 0.68 Å, respectively. The formed hydrogen bonds are shown as green dotted lines.

−18.55 kcal/mol, with RMSD range of 0.90−4.41 Å;moreover, they exhibit up to four hydrogen bonds.

The analysis of the aforementioned docking results reveals that there is a direct reasonable correlation between the AutoDock binding free energy (ΔG_b,kcal/mol) and the MAO-A inhibitory activity (K_i,pM), being of correlation coefficients (R^2) of 0.788 for compounds (**1b**), (**2b**,**d**), (**3a**,**e**,**g**), (**4b**), (**5a**,**b**), (**7a**,**b**), (**8c**), (**9d**), and (**10a**), as illustrated in Figure 2A. Additionally, the coumarin analogues (**2c**) and (**1b**) were docked into MAO-A receptor, where they fit similarly within the binding site, revealing high binding affinity (ΔG_b) of −17.10 and −16.95 kcal/mol, respectively. These docking results are highly correlated to their biological ones, where their MAO-A inhibitory activities are 11.0 and 5.01 pM and their in vivo ED_{50} are 7.95 and 9.14 nM, respectively.

As shown in Figure 3, compound (**2c**) was docked exhibiting four hydrogen bonds between its O (pyrone), 2-C═O,and SH with OH of Tyr444, NH of Asn181,and C═O of Ala111,

dx.doi.org/10.1021/jm301014y | J. Med. Chem. 2012, 55, 10424−10436

Table 4. The Best Results of the Flexible Docking Regarding the Binding Free Energies (ΔG_b) and Inhibition Constants (K_i) of Compounds Docked into MAO-B, the Distances and Angles of Hydrogen Bonds between Compounds and Amino Acids Involved in MAO-B and RMSD from Co-crystallized XCG Native Ligand

			hydrogen bonds between atoms of compounds and amino acids of MAO-B				
compd	ΔG_b[a] (kcal/mol)	K_i[b] (pM)	atom of compd	amino acid	distance (Å)	angle (deg)	RMSD[c] (Å)
2a	−13.13	238.08	2C═O	HO of Tyr435	1.95	152.9	5.44
			SH (terminal)	O═C of Pro102	2.16	131.7	
2c	−13.84	71.74	O (pyrone)	HO of Tyr326	1.95	139.1	3.18
			N−N (thiadiazole)	HS of Cys172	2.15	132.0	
			N−N (thiadiazole)	HS of Cys172	2.01	142.8	
			SH (terminal)	O═C of Leu171	2.31	150.7	
2d	−12.72	478.14	terminal SH	O═C of Pro102	2.07	169.3	4.56
3c	−13.30	177.24	2C═O	HN of Asn203	2.21	132.7	2.70
			N−N (thiadiazole)	HO of Tyr326	2.19	152.7	
			C−S (side chain)	HO of Tyr326	2.49	126.7	
3h	−13.08	259.64	thiadiazole C═N	HO of Ser200	1.78	146.1	4.15
			morpholine O	HN of Arg100	2.10	115.9	
4a	−12.69	500.54	O (side chain)	HN of Thr201	2.25	144.1	4.51
5b	−12.65	529.61	*d*	*d*	*d*	*d*	4.71
6b	−13.22	203.74	thiazolidinone 5C═O	HN of Gly101	2.20	161.5	5.16
			−CONH	O═C of Gly101	1.82	110.3	
			−HNCO	HN of Thr201	2.35	147.3	
7a	−14.33	31.18	2-C═O	HO of Tyr435	2.30	128.1	3.58
			2-C═O	HS of Cys172	2.33	115.6	
			O (pyrone)	HS of Cys172	2.00	127.8	
			N−N (triazole)	HO of Tyr326	1.89	136.0	
7b	−14.42	27.00	triazole C═N	HO of Tyr326	2.46	129.5	4.55
			triazole C═N−N	HO of Tyr326	2.04	116.9	
8c	−12.51	681.54	2C═O	HN of Gly101	2.41	152.5	3.67
			O (pyrone)	HN of Gly101	2.19	149.4	
9a	−14.05	50.28	2C═O	HN of Asn203	1.93	168.2	5.29
9b	−14.81	14.03	2C═O	HN of Arg100	2.14	133.4	5.13
			O (pyrone)	HN of Gly101	2.02	169.3	
			−CONH	O═C of Pro102	2.23	112.8	
			−HNCO	HO of Tyr326	2.15	126.0	
9c	−14.31	32.52	O (pyrone)	HN of Gly101	2.20	140.2	4.73
			7-O	HN of Thr201	2.38	135.1	
9d	−13.57	113.55	7-O	HN of Thr201	2.36	131.1	4.92
XCG[e]	−12.06	1460	NH (imidazole)	O═C of Pro102	2.00	149.8	0.68

[a]Binding free energy. [b]Inhibition constant. [c]Root mean square deviation. [d]No hydrogen bond detected. [e]HRM: 7-methoxy-1-methyl-9*H*-*β*-carboline.

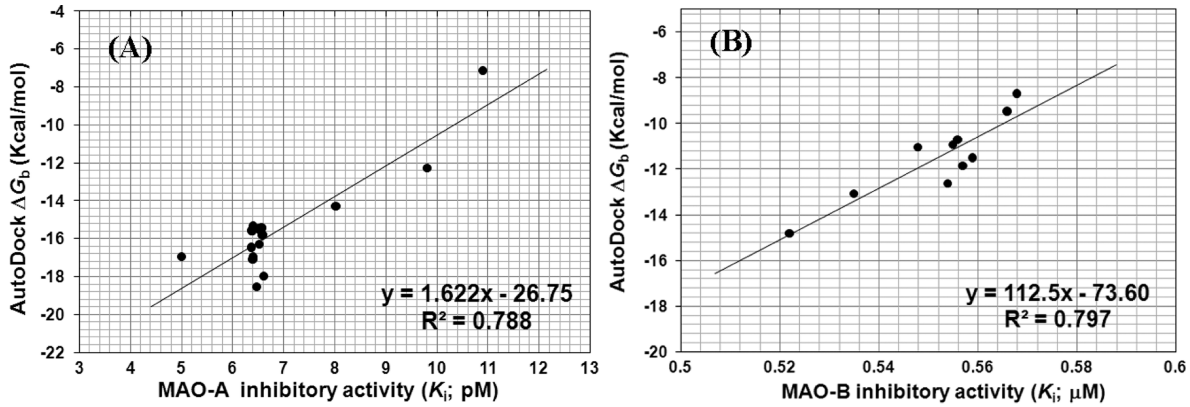

Figure 2. Correlation between MAO-A inhibitory activity (K_i, pM) and AutoDock ΔG_b (A) for compounds (**1b**), (**2b,d**), (**3a,e,g**), (**4b**), (**5a,b**), (**7a,b**), (**8c**), (**9d**), and (**10a**) and between MAO-B inhibitory activity (K_i, μM) and AutoDock ΔG_b (B) for compounds (**3a,b,e,h**), (**5b**), (**6a**), (**8a,d**), (**9b**), and (**10b**), revealing direct relationship of correlation coefficients (R^2) being 0.788 and 0.797, respectively.

within RMSD of 1.05 Å, also compound (**1b**) is bound through four hydrogen bonds between its 2-C═O and terminal NH_2 with exactly the same amino acids involved in binding of compound (**2c**), within RMSD of 1.51 Å.

dx.doi.org/10.1021/jm301014y | *J. Med. Chem.* 2012, 55, 10424−10436

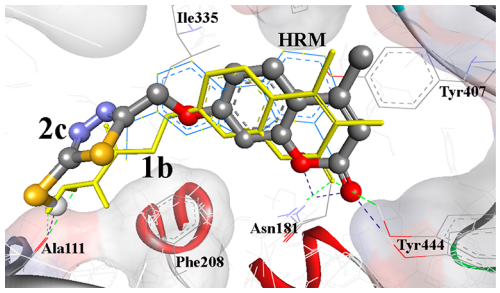

Figure 3. Mode of binding of compound (**2c**) (ball and stick, colored by element) and compound (**1b**) (yellow sticks) involving flexible docking into the binding pocket of MAO-A (2Z5X) shown as solid backbone ribbon with the HRM ligand (blue lines) The hydrogen bonds are shown as blue and green dashed lines for compound (**2c**) and (**1b**), respectively.

On the other hand, the flexible docking into MAO-B macromolecule is represented in Table 4, where many compounds reveal fairly good docking results in comparison to the natively embedded cocrystallized ligand. The promising compounds as drug candidates include compounds: (**9b**), (**7b**), (**7a**), (**9c**), (**9a**), (**2c**), (**9d**), (**3c**), (**6b**), (**2a**), and (**3h**), which reveal binding free energies (ΔG_b) within the range of −13.08 to −14.8 kcal/mol, with RMSD range of 2.70−5.44 Å; moreover, they exhibit up to four hydrogen bonds.

The biologically active target compounds (**9b**) and (**3h**), which have almost the same inhibitory activities against MAO-B, being of 0.522 and 0.535 μM and in vivo ED_{50} of 74.58 and 75.74 μM, respectively, exhibited low binding free energies (ΔG_b) being of −14.81 and −13.08 kcal/mol, respectively, upon their docking into MAO-B as shown in detail in Figure 4

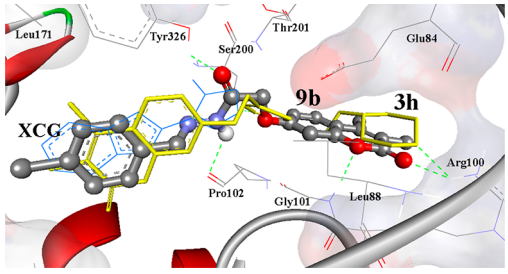

Figure 4. AutoDock binding affinities of compounds (**9b**) (ball and stick, colored by element) and (**3h**) (yellow sticks) into MAO-B (2XFN). The docked inhibitors seem exactly overlapped onto the native XCG ligand (blue lines). The binding MAO-B pocket is shown in solid surface and the hydrogen bonds as green dotted lines.

in comparison to the bound native ligand **2**. Compound (**9b**) exhibits four hydrogen bonds between its moieties and amino acids: Arg100, Gly101, Prp102, and Tyr326, within RMSD of 5.13 Å, whereas compound (**3h**) binds by two hydrogen bonds between its thiazole (C═N) and morpholine (O) with amino acids: Arg100 and Ser200, within RMSD of 4.15 Å.

The analysis of the docking results, revealed a direct reasonable correlation between the AutoDock binding free energy (ΔG_b; kcal/mol) and the MAO-B inhibitory activity (μM), being of better correlation coefficients (R^2) of 0.797 for compounds (**3a,b,e,h**), (**5b**), (**6a**), (**8a,d**), (**9b**), and (**10b**), as illustrated in Figure 2B.

Additionally, the results of the in vivo MAO inhibiting properties (ED_{50}) of the compounds studied involving the in vivo tryptamine seizure potentiation procedure in rats, revealed direct correlation as shown in Figures 5 and 6, where

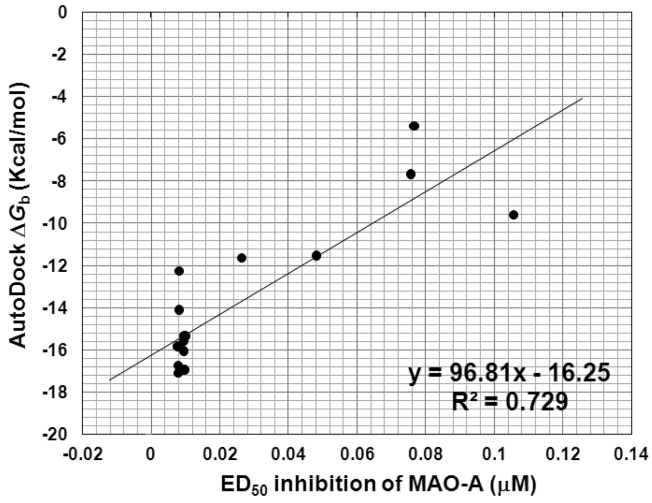

Figure 5. Correlation between in vivo ED_{50} inhibition of MAO-A (μM) and AutoDock ΔG_b for compounds (**1a,b**), (**2a,c,d**), (**3c,f,g,h**), (**5a**), (**6a**), (**7a**), (**8a,c,d**), and (**10b**), revealing a reasonable direct correlation coefficients (R^2) being 0.729.

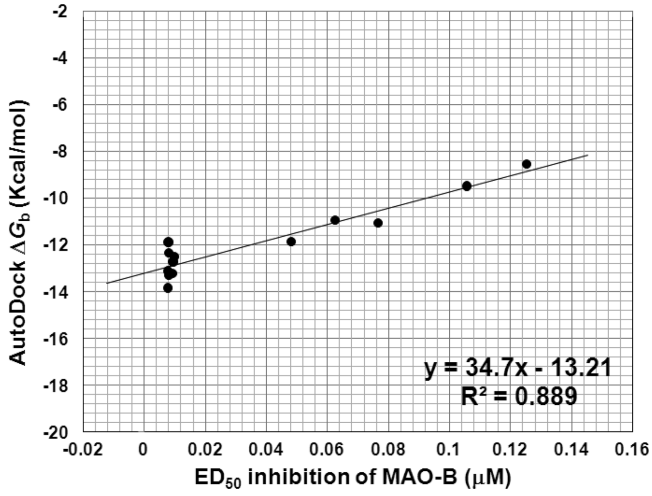

Figure 6. Correlation between in vivo ED_{50} inhibition of MAO-B (μM) and AutoDock ΔG_b for compounds (**1a**), (**2a,c,d**), (**3b,c**), (**6a,b**), (**8a,b,c**), and (**10a,b**), revealing excellent direct relationship of correlation coefficients (R^2) of 0.889.

correlation between the in vivo ED_{50} inhibition of MAO-A (μM) and the AutoDock ΔG_b (kcal/mol) for compounds (**1a,b**), (**2a,c,d**), (**3c,f,g,h**), (**5a**), (**6a**), (**7a**), (**8a,c,d**), and (**10b**) exhibits highly reasonable direct correlation coefficients (R^2) of 0.729 (Figure 5). To a better extent, the correlation between the ED_{50} inhibition of MAO-B (μM) and the AutoDock ΔG_b for compounds (**1a**), (**2a,c,d**), (**3b,c**), (**6a,b**), (**8a,b,c**), and (**10a,b**) exhibits excellent direct correlation coefficients (R^2) being of 0.889 as shown in Figure 6.

Being that the correlation (R^2) between ΔG_b and MAO-A inhibition, is 0.788 and (R^2) between ΔG_b and ED_{50} of MAO-A is 0.729, the aforementioned reasonable correlations between the molecular simulation and biological MAO-A inhibition, implied that acetohydrazide (**1b**), 5-mercapto-1,3,4-thiadiazole (**2d**), 5-(2-morpholinoethylthio)-1,3,4-thiadiazole (**3g**), 5-(4-

dx.doi.org/10.1021/jm301014y | J. Med. Chem. 2012, 55, 10424−10436

chlorophenylamino)-1,3,4-thiadiazole (**5a**), 4-(4-chlorophenyl)-5-mercapto-4*H*-1,2,4-triazole (**7a**), and 5-(2-morpholinoethylthio)-4-(4-chlorophenyl)-4*H*-1,2,4-triazole (**8c**) represent to a higher extent the structural prerequisites for the design of potentially active MAO-A inhibitors.

On the other hand, ΔG_b and MAO-B inhibition are correlated by (R^2) of 0.797; moreover, ΔG_b is correlated with ED_{50} of MAO-B by (R^2) of 0.889. These reasonable correlations between the molecular simulation and the biological MAO-B inhibition indicated that 5-(2-(diethylamino)ethylthio)-1,3,4-oxadiazol (**3b**), *N*-(2-(4-chlorophenylimino)-4-oxothiazolidin-3-yl)acetamide (**6a**), 5-(2-(diethylamino)ethylthio)-4-(4-chlorophenyl)-4*H*-1,2,4-triazole (**8a**), and *N*-(2-(4-chlorophenyl)-4-oxothiazolidin-3-yl)-acetamide (**10b**) represent to a higher extent the structural prerequisites for designing potentially active MAO-B inhibitors.

Structure–Activity Relationship (SAR). According to the molecular simulation results, a significant to mild nonselective increase of MAO-A and MAO-B inhibitory affinity of both mercapto-1,3,4-oxadiazole (**2b**) and their thiadiazole bioisosters (**2c,d**) than the parent hydrazide lead (**1a**) is observed by replacing acetohydrazide by 5-mercapto-1,3,4-oxadiazole or 1,3,4-thiadiazole. Also a mild increase is observed by introducing 4-chlorophenylthiosemicarbazides in (**4a,b**) and 4-(4-chlorophenyl)-5-mercapto-1,2,4-triazoles in (**7a,b**) and Schiff's bases (**9a–d**). The above-mentioned increase of the inhibitory affinities may be attributed to the inserted aryl fragment of (**2b,c,d**) and (**7a,b**), which tend to be deeply embedded and accommodated into the hydrophobic region of MAO isoenzymes, exhibiting an electrostatic surface attraction and hydrophobic interactions with their active sites. While such affinity increase of compounds (**4a,b**) and (**9a,d**) may be attributed to their flexible thiosemicarbazides (**4a,b**), benzylidene acetohydrazide (**9a**), or ethylidene acetohydrazide (**9d**) which enable them to hydrophilically interact with more hydrogen binding. The isosteric changes of 2-(4-chlorophenylimino)-4-oxothiazolidine congener (**6b**) afford a slight enhanced MAO-B selective affinity over MAO-A. The aforementioned docking results matched well with the biological results (Table 1).

Isosteric variations in position 7 of the studied coumarin derivatives restored satisfactory MAO inhibitory affinity and MAO-A/MAO-B selectivity. The results considering SAR reveal that the higher MAO isoenzymes binding affinities are obtained with the structure features; 4-methyl or 3,4-dimethyl-7-oxycoumarin, 4-methylcoumarinylthiosemicarbazide, and *N*′-(4-chlorobenzylidene) acetohydrazide Schiff's base, whereas such affinity is dropped by the directly attached 4-chlorophenyl group to the thaizolidinone ring of the 4-methylcoumarinyl-7-oxyacetamide derivative, by the oxadiazole fragment and rarely by the thiadiazole moiety.

The higher affinity of the studied coumarin analogues to MAO-A being much more than MAO-B can be explained by:

(i) The structural differences arising from Ile-335 in MAO-A vs Tyr-326 in MAO-B, where the compounds could not be accommodated into MAO-B because of their structural overlap with Tyr-326.

(ii) The active site cavity of MAO-A Phe208 residue was located at the position occupied by Ile199 in MAO-B. As a result, a $\pi-\pi$ interaction between the studied compounds and Phe208 significantly enhances their affinities to MAO-A. While, such interaction is absent between the compounds and Ile199 in MAO-B. Loss of this interaction may explain the weaker MAO-B binding affinities compared to MAO-A ones.

(iii) The major structural dissimilarity is that MAO-A has a monopartite substrate cavity of ∼550 Å^3 volume and MAO-B contains a dipartite cavity structure with volumes of ∼290 Å^3 (hydrophobic entrance cavity) and ∼400 Å^3 (polar substrate cavity). This means that MAO-B inhibitors of high affinities must undergo polar and apolar interactions with the substrate and entrance cavities, respectively. However, such prerequisites are not available in the studied coumarins, which have mainly hydrophobic moieties being of 2-oxo-2*H*-chromene aromatic structure and side chains being: acetohydrazides, 4-chlorophenylamino, 5-(2-(diethylamino)-ethylthio) oxadiazoles, 5-(2-morpholinoethylthio) analogues of oxadiazoles, thiadiazoles, and triazoles, whereas the hydrophilic side chain containing compounds such as thiosemicarbazide (**4a**) or acetohydrazide (**9a–c**) can reveal some fitting into MAO-B.

CONCLUSION

New series of bioactive 7-oxycoumarin derivatives were designed, synthesized, and evaluated for their in vitro MAO inhibitory activity regarding the two isoforms of the enzyme. All the studied compounds show a very high affinity and selectivity for the MAO-A isoenzyme, compared to clorgyline and moclobemide, with K_i values in the picomolar concentration range. In particular, the acetohydrazide derivative (**1b**) (K_i (MAO-A) = 5.01 pM, and SI = 9.66 × 10^4) and the diethylaminoethylthio-1,3,4-thiadiazole compound (**3d**) (K_i (MAO-A) = 5.18 pM, and SI = 9.58 × 10^4) are exceptionally the most potent and selective MAO-A inhibitors. In addition, most of the target compounds display high potency toward MAO when tested in vivo. Both 5-mercapto-1,3,4-oxadiazole (**2a**) and its thiadiazole bioisoster (**2c**) display the highest potencies the in vivo (ED_{50} = 7.85 and 7.95 nM respectively). In addition, the docking studies performed on these compounds reveal that there is a direct reasonable correlation between the AutoDock binding free energy (ΔG_b, kcal/mol) and the MAO-A inhibitory activity (K_i, pM), being of correlation coefficients (R^2) of 0.788 for compounds (**1b**), (**2b,d**), (**3a,e,g**), (**4b**), (**5a,b**), (**7a,b**), (**8c**), (**9d**), and (**10a**). Compound (**1b**) is bound through four hydrogen bonds between its 2-C=O and terminal NH_2 with OH of Tyr444, NH of Asn181, and C=O of Ala111 within RMSD of 1.51 Å., Additionally, the results of in vivo MAO inhibiting properties (ED_{50}) of compounds studied involving in vivo tryptamine seizure potentiation procedure in rats reveal a direct correlation, where a correlation between the in vivo ED_{50} inhibition of MAO-A (μM) and the AutoDock ΔG_b (kcal/mol) for compounds (**1a,b**), (**2a,c,d**), (**3c,f,g,h**), (**5a**), (**6a**), (**7a**), (**8a,c,d**), and (**10b**) exhibits highly reasonable direct correlation coefficients (R^2) of 0.729. Isosteric variations in position 7 of the studied coumarin derivatives restore a satisfactory MAO inhibitory affinity and MAO-A/MAO-B selectivity. The results considering SAR reveal that the higher MAO isoenzymes binding affinities were obtained with the structure features: 4-methyl or 3,4-dimethyl-7-oxycoumarin, 4-methylcoumarinylthiosemicarbazide, *N*′-(4-chlorobenzylidene) acetohydrazide Schiff's base, whereas such affinity is dropped by the directly attached 4-chlorophenyl group to the thaizolidinone ring of 4-

methylcoumarinyl-7-oxyacetamide derivative, by the oxadiazole fragment, and rarely by the thiadiazole moiety.

EXPERIMENTAL SECTION

Chemistry. Melting points were determined on Electrothermal IA 9000 apparatus and were uncorrected. The infrared (IR) spectra were recorded using Nexus 670 FT-IR FT-Raman spectrometer as potassium bromide discs at the National Research Centre. The proton nuclear resonance (^{1}H NMR) spectra were determined on Varian mercury 500 MHz spectrometer, using tetramethylsilane (TMS) as the internal standard, at the National Research Centre. The mass spectra were performed on JEOL JMS-AX500 mass spectrometer at the National Research Centre. The reactions were followed by TLC (silica gel, aluminum sheets 60 F254, Merck) using chloroform−methanol (9.5:0.5 v/v) as eluent and sprayed with iodine−potassium iodide reagent. The purity of the newly synthesized compounds was assessed by TLC and elemental analysis and was found to be higher than 95%.

Preparation of 2-(4-Methyl (and/or 3,4-Dimethyl)-2-oxo-2*H*-chromen-7-yloxy) Acetohydrazides (1a,b). Acetohydrazides (**1a**)[28] and (**1b**)[29] were prepared according to the reported methods.

Preparation of 7-[(5-Mercapto-1,3,4-oxadiazol-2-yl)-methoxy]-4-methyl (and/or 3,4-Dimethyl) coumarin (2a,b). Compounds (**2a**)[27] and (**2b**) were prepared according to Eid et al.[27]

7-((5-Mercapto-1,3,4-oxadiazol-2-yl)methoxy)-3,4-dimethyl-2*H*-chromen-2-one (2b). Yield 72%; mp 220−5 °C; mol wt 304.32. Crystallization: EtOH. IR (cm^{-1}, KBr): 3089 (CH aromatic stretching), 2926 (CH aliphatic stretching), 2610 (SH), 1693 (C═O, α-pyrone). ^{1}H NMR (DMSO-d_6, δ, ppm): 2.22 (3H, s, CH_3), 2.33 (3H, s, CH_3), 3.01 (1H, s, SH, D_2O exchangeable), 5.41 (2H, s, OCH_2), 6.83−7.55 (3H, m, Ar−H). MS *m*/*z* (RA %): 305 (M^+ + 1) (13%), 304 (M^+) (69%), 190 (100%), 162 (66%), 147 (16%).

Preparation of 7-[(5-Mercapto-1,3,4-thiadiazol-2-yl)-methoxy]-4-methyl (and/or 3,4-Dimethyl)coumarins (2c,d). Compounds (**2c**)[27] and (**2d**) were prepared according to the reported method.[27]

7-((5-Mercapto-1,3,4-thiadiazol-2-yl)methoxy)-3,4-dimethyl-2*H*-chromen-2-one (2d). Yield 78%; mp 260−5 °C; mol wt 320.39. Crystallization: EtOH. IR (cm^{-1}, KBr): 3071 (CH aromatic stretching), 2874 (CH aliphatic stretching), 2667 (SH), 1671 (C═O, α-pyrone). ^{1}H NMR (DMSO-d_6, δ, ppm): 2.21 (3H, s, CH_3), 2.31 (3H, s, CH_3), 3.01 (1H, s, SH, D_2O exchangeable), 5.38 (2H, s, OCH_2), 6.82−7.56 (3H, m, Ar−H). MS *m*/*z* (RA %): 320 (M^+) (3%), 248 (61%), 220 (25%), 190 (46%), 161 (100%), 147 (32%).

General Procedure for Preparation of 7-((5-(2-(Diethylamino)-ethylthio (and/or 2-Morpholinoethylthio)-1,3,4-oxadiazol (and/or 1,3,4-Thiadiazol)-2-yl)methoxy)-4-methyl (and/or 3,4-Dimethyl)-2*H*-chromen-2-ones (3a−h). A mixture of (**2a−d**) (0.01 mol), diethylaminoethyl chloride hydrochloride, and/or 4-(2-chloroethyl)morpholine hydrochloride (0.03 mol) and anhydrous potassium carbonate (4.2 g, 0.03 mol) in dry acetone (100 mL) was refluxed while stirring for 10−15 h. The mixture was filtered while hot, the filtrate was concentrated, and water was added to precipitate the desired target compounds which were recrystallized from acetone/water.

7-((5-(2-(Diethylamino)ethylthio)-1,3,4-oxadiazol-2-yl)-methoxy)-4-methyl-2*H*-chromen-2-one (3a). Yield 67%; mp 91−3 °C; mol wt 389.47. IR (cm^{-1}, KBr): 3067 (CH aromatic stretching), 2967, 2932 (CH aliphatic stretching), 1728 (C═O, α-pyrone). ^{1}H NMR (DMSO-d_6, δ, ppm): 1.07 (6H, t, 2 $\underline{CH_3}CH_2$), 2.39 (3H, s, CH_3), 2.67 (4H, q, 2 $\underline{CH_2}CH_3$), 2.94 (2H, t, CH_2N), 3.45 (2H, t, CH_2S), 5.26 (2H, s, OCH_2), 6.16 (1H, s, H-3 coumarin), 6.92−7.53 (3H, m, Ar−H). MS *m*/*z* (RA %): 390 (M^+ + 1) (12%), 211(13%), 174 (15%), 145 (45%), 98 (100%).

7-((5-(2-(Diethylamino)ethylthio)-1,3,4-oxadiazol-2-yl)-methoxy)-3,4-dimethyl-2*H*-chromen-2-one (3b). Yield 65%; mp 78−80 °C; mol wt 403.50. IR (cm^{-1}, KBr): 3065 (CH aromatic stretching), 2967, 2925 (CH aliphatic stretching), 1714 (C═O, α-pyrone). ^{1}H NMR (DMSO-d_6, δ, ppm): 1.00 (6H, t, 2 $\underline{CH_3}CH_2$), 2.15 (3H, s, CH_3), 2.34 (3H, s, CH_3), 2.56 (4H, q, 2 $\underline{CH_2}CH_3$), 2.83(2H, t, CH_2N), 3.41 (2H, t, CH_2S), 5.23 (2H, s, OCH_2), 6.87−7.50 (3H, m, Ar−H). MS *m*/*z* (RA %): 404 (M^+ + 1) (18%), 190 (5%), 161 (16%), 145 (6%), 99 (100%).

7-((5-(2-(Diethylamino)ethylthio)-1,3,4-thiadiazol-2-yl)-methoxy)-4-methyl-2*H*-chromen-2-one (3c). Yield 76%; mp 175−7 °C; mol wt 405.53. IR (cm^{-1}, KBr): 3073 (CH aromatic stretching), 2973, 2937 (CH aliphatic stretching), 1716 (C═O, α-pyrone). ^{1}H NMR (DMSO-d_6, δ, ppm): 1.17 (6H, t, 2 $\underline{CH_3}CH_2$), 2.37 (3H, s, CH_3), 3.12 (4H, q, 2 $\underline{CH_2}CH_3$), 3.40 (2H, t, CH_2N), 3.97 (2H, t, CH_2S), 5.67 (2H, s, OCH_2), 6.23 (1H, s, H-3 coumarin), 7.06−7.71 (3H, m, Ar−H). MS *m*/*z* (RA %): 405 (M^+) (2%), 214 (12%), 150 (19%), 149 (18%), 148 (100%).

7-((5-(2-(Diethylamino)ethylthio)-1,3,4-thiadiazol-2-yl)-methoxy)-3,4-dimethyl-2*H*-chromen-2-one (3d). Yield 77%; mp 78−81 °C; mol wt 419.56. IR (cm^{-1}, KBr): 3062 (CH aromatic stretching), 2967, 2927 (CH aliphatic stretching), 1717 (C═O, α-pyrone). ^{1}H NMR (DMSO-d_6, δ, ppm): 1.18 (6H, t, 2 $\underline{CH_3}CH_2$), 2.20 (3H, s, CH_3), 2.38 (3H, s, CH_3), 3.20 (4H, q, 2 $\underline{CH_2}CH_3$), 2.50 (2H, t, CH_2N), 3.89 (2H, t, CH_2S), 5.48 (2H, s, OCH_2), 6.89−7.56 (3H, m, Ar−H). MS *m*/*z* (RA %): 420 (M^+ + 1) (6%), 173 (6%), 162 (3%), 99 (33%), 86 (100%).

7-((5-(2-Morpholinoethylthio)-1,3,4-oxadiazol-2-yl)-methoxy)-4-methyl-2*H*-chromen-2-one (3e). Yield 70%; mp 93−5 °C; mol wt 403.45. IR (cm^{-1}, KBr): 3069 (CH aromatic stretching), 2957, 2833 (CH aliphatic stretching), 1727 (C═O, α-pyrone). ^{1}H NMR (DMSO-d_6, δ, ppm): 2.39 (3H, s, CH_3), 2.50 (4H, t, 2 CH_2 N morpholine), 2.77 (2H, t, CH_2N), 3.44 (2H, t, CH_2S), 3.68 (4H, t, 2 CH_2O morpholine), 5.27 (2H, s, OCH_2), 6.17 (1H, s, H-3 coumarin), 6.93−7.54 (3H, m, Ar−H). MS *m*/*z* (RA %): 403 (M^+) (0.2%), 189 (2%), 176 (2%), 147 (6%), 113 (16%), 18(100%).

7-((5-(2-Morpholinoethylthio)-1,3,4-oxadiazol-2-yl)-methoxy)-3,4-dimethyl-2*H*-chromen-2-one (3f). Yield 71%; mp 109−110 °C; mol wt 417.48. IR (cm^{-1}, KBr): 3074 (CH aromatic stretching), 2930, 2861 (CH aliphatic stretching), 1703 (C═O, α-pyrone). ^{1}H NMR (DMSO-d_6, δ, ppm): 2.22 (3H, s, CH_3), 2.34 (3H, s, CH_3), 2.51 (4H, t, 2 CH_2 N morpholine), 2.72 (2H, t, CH_2N), 3.40 (2H, t, CH_2S), 3.65 (4H, t, 2 CH_2O morpholine), 5.25 (2H, s, OCH_2), 6.92−7.55 (3H, m, Ar−H). MS *m*/*z* (RA %): 417 (M^+) (2%), 189 (3%), 161 (7%), 113 (43%), 100 (100%), 98 (12%).

7-((5-(2-Morpholinoethylthio)-1,3,4-thiadiazol-2-yl)-methoxy)-4-methyl-2*H*-chromen-2-one (3g). Yield 67%; mp 250−3 °C; mol wt 419.52. IR (cm^{-1}, KBr): 3065 (CH aromatic stretching), 2976, 2881 (CH aliphatic stretching), 1719 (C═O, α-pyrone). ^{1}H NMR (DMSO-d_6, δ, ppm): 2.37 (3H, s, CH_3), 2.60 (4H, t, 2 CH_2 N morpholine), 2.64 (2H, t, CH_2N), 3.45 (2H, t, CH_2S), 3.49 (4H, t, 2CH_2O morpholine), 5.65 (2H, s, OCH_2), 6.23 (1H, s, H-3 coumarin), 7.03−7.70 (3H, m, Ar−H). MS *m*/*z* (RA %): 419 (M^+) (1%), 359 (4%), 187 (4%), 176 (7%), 147 (34%), 28 (100%).

7-((5-(2-Morpholinoethylthio)-1,3,4-thiadiazol-2-yl)-methoxy)-3,4-dimethyl-2*H*-chromen-2-one (3h). Yield 70%; mp 140−2 °C; mol wt 433.54. IR (cm^{-1}, KBr): 3052 (CH aromatic stretching), 2966, 2924 (CH aliphatic stretching), 1717 (C═O, α-pyrone). ^{1}H NMR (DMSO-d_6, δ, ppm): 2.03 (3H, s, CH_3), 2.33 (3H, s, CH_3), 2.35 (4H, t, 2 CH_2 N morpholine), 2.61 (2H, t, CH_2N), 3.40 (2H, t, CH_2S), 3.47 (4H, t, 2 CH_2O morpholine), 5.60 (2H, s, OCH_2), 6.99−7.68 (3H, m, Ar−H). MS *m*/*z* (RA %): 433 (M^+) (2%), 288 (7%), 189 (7%), 161 (27%), 113 (60%), 100 (100%).

General Procedure for Preparation of 1-(2-(4-Methyl (and/or 3,4-Dimethyl)coumarinyl-7-yloxy)acetyl)-4-(4-chlorophenyl) Thiosemicarbazides(4a,b). Compounds (**4a**)[30] and (**4b**) were prepared according to the reported method.[30]

1-(2-(3,4-Dimethyl-2-oxo-2*H*-chromen-7-yloxy)acetyl)-4-(4-chloro phenyl) Thiosemicarbazide (4b). Yield 88%; mp 207−9 °C; mol wt 431.89. Crystallization: AcOH. IR (cm^{-1}, KBr): 3399, 3315 (NH), 3110 (CH aromatic stretching), 2962 (CH aliphatic stretching), 1702 (C═O, α-pyrone), 1670 (C═O), 1242 (C═S). ^{1}H NMR (DMSO-d_6, δ, ppm): 1.99 (1H, s, NH, D_2O exchangeable), 2.05 (3H, s, CH_3), 2.34 (3H, s, CH_3), 3.82 (1H, s, NH, D_2O exchangeable), 5.23 (2H, s, OCH_2), 6.83−7.60 (7H, m, Ar−H), 7.98 (1H, s, NH, D_2O exchangeable). MS *m*/*z* (RA %): 433 (M^+ + 2) (3%), 431 (M^+) (10%), 429 (9%), 190 (88%), 189 (64%), 161 (100%).

dx.doi.org/10.1021/jm301014y | J. Med. Chem. 2012, 55, 10424−10436

General Procedure for Preparation of 7-((5-(4-Chlorophenylamino)-1,3,4-thiadiazol-2-yl)methoxy)-4-methyl (and/or 3,4-Dimethyl)coumarins (5a,b). Compounds (**5a**)[30] and (**5b**) were prepared according to the reported method.[30]

7-((5-(4-Chlorophenylamino)-1,3,4-thiadiazol-2-yl)-methoxy)-3,4-dimethyl-2*H*-chromen-2-one (5b). Yield 88%; mp 207−9 °C; mol wt 413.88. Crystallization: AcOH. IR (cm^{-1}, KBr): 3303 (NH), 3077 (CH aromatic stretching), 2926 (CH aliphatic stretching), 1676 (C═O, α-pyrone). ^{1}H NMR (DMSO-d_6, δ, ppm): 2.03 (3H, s, CH_3), 2.32 (3H, s, CH_3), 5.49 (2H, s, OCH_2), 7.09−7.67 (7H, m, Ar−H), 10.58 (1H, s, NH, D_2O exchangeable). MS *m*/*z* (RA %): 415 (M^+ + 2) (4%), 413 (M^+) (12%), 226 (30%), 191 (30%), 190 (100%), 162 (91%).

Preparation of *N*-(2-(4-Chlorophenylimino)-4-oxothiazolidin-3-yl)-2-(4-methyl (and/or 3,4-Dimethyl)coumarin-7-yloxy)-acetamides (6a,b). A mixture of thiosemicarbazides (**4a,b**) (0.01 mol), chloroacetic acid (0.01 mol), and anhydrous sodium acetate (0.5 g) in absolute ethanol was refluxed while stirring for about 25 h. The solution was concentrated, and the precipitated solid was filtered and crystallized from acetic acid/water.

***N*-(2-(4-Chlorophenylimino)-4-oxothiazolidin-3-yl)-2-(4-methyl-2-oxo-2*H*-chromen-7-yloxy)acetamide (6a).** Yield 76%; mp 225−7 °C; mol wt 457.89. IR (cm^{-1}, KBr): 3225 (NH), 3071 (CH aromatic stretching), 2960 (CH aliphatic stretching), 1723 (C═O, α-pyrone), 1665 (C═O). ^{1}H NMR (DMSO-d_6, δ, ppm): 2.33 (3H, s, CH_3), 3.75 (2H, s, CH_2-thiazolidinone), 5.18 (2H, s, OCH_2), 6.17 (1H, s, H-3 coumarin), 6.83−7.58 (7H, m, Ar−H), 10.58 (1H, s, NH, D_2O exchangeable). MS *m*/*z* (RA %): 459 (M^+ + 2) (12%), 457 (M^+) (36%), 443 (25%), 341 (33%), 206 (31%), 50 (100%).

***N*-(2-(4-Chlorophenylimino)-4-oxothiazolidin-3-yl)-2-(3,4-dimethyl-2-oxo-2*H*-chromen-7-yloxy)acetamide (6b).** Yield 74%; mp 170−2 °C; mol wt 471.91. IR (cm^{-1}, KBr): 3290 (NH), 3095 (CH aromatic stretching), 2921 (CH aliphatic stretching), 1705 (C═O, α-pyrone), 1609 (C═O). ^{1}H NMR (DMSO-d_6, δ, ppm): 2.03 (3H, s, CH_3), 2.30 (3H, s, CH_3), 3.69 (2H, s, CH_2-thiazolidinone), 5.16 (2H, s, OCH_2), 6.81−7.63 (7H, m, Ar−H), 10.40 (1H, s, NH, D_2O exchangeable). MS *m*/*z* (RA %): 473 (M^+ + 2) (2%), 471 (M^+) (6%), 268 (10%), 224 (24%), 147 (36%), 55(91%).

General Procedure for Preparation of 7-[(4-(4-Chlorophenyl)-5-mercapto-1,2,4-triazol-3-yl)methoxy]-4-methyl (and/or 3,4-Dimethyl) Coumarins (7a,b). Compounds (**7a**)[30] and (**7b**) were prepared according to the reported method.[30]

7-((4-(4-Chlorophenyl)-5-mercapto-4*H*-1,2,4-triazol-3-yl)-methoxy)-3,4-dimethyl-2*H*-chromen-2-one (7b). Yield 88%; mp 220−2 °C; mol wt 413.88. Crystallization: EtOH. IR (cm^{-1}, KBr): 3093 (CH aromatic stretching), 2920 (CH aliphatic stretching), 2550 (SH), 1685 (C═O, α-pyrone). ^{1}H NMR (DMSO-d_6, δ, ppm): 2.17 (3H, s, CH_3), 2.35 (3H, s, CH_3), 3.01 (1H, s, SH, D_2O exchangeable), 5.08 (2H, s, OCH_2), 6.77−7.49 (7H, m, Ar−H). MS *m*/*z* (RA %): 415 (M^+ + 2) (9%), 413 (M^+) (24%), 190 (100%), 162 (26%), 147 (7%).

General Procedure for Preparation of 7-((5-(2-(Diethylamino)ethylthio) (and/or (2-Morpholinoethylthio))-4-(4-chlorophenyl)-4*H*-1,2,4-triazol-3-yl) methoxy)-4-methyl (and/or 3,4-Dimethyl) Coumarins (8a−d). The target compounds (**8a−d**) were prepared from (**7a,b**) according to the previously described method for the preparation of compounds (**3a−h**), and the synthesized compounds were crystallized from acetone/water.

7-((5-(2-(Diethylamino)ethylthio)-4-(4-chlorophenyl)-4*H*-1,2,4-triazol-3-yl)methoxy)-4-methyl-2*H*-chromen-2-one (8a). Yield 70%; mp 115−7 °C; mol wt 499.02. IR (cm^{-1},KBr): 3088 (CH aromatic stretching), 2966, 2932 (CH aliphatic stretching), 1741(C═O, α-pyrone). ^{1}H NMR (DMSO-d_6, δ, ppm): 1.01 (6H, t, 2 $\underline{CH_3}CH_2$), 2.34 (3H, s, CH_3), 2.41 (4H, q, 2 $\underline{CH_2}CH_3$), 2.47 (2H, t, CH_2N), 3.27 (2H, t, CH_2S), 5.21 (2H, s, OCH_2), 6.19 (1H, s, H-3 coumarin), 6.83−7.60 (7H, m, Ar−H). MS *m*/*z* (RA %): 501 (M^+ + 2) (20%), 499 (M^+) (60%), 427 (67%), 398 (60%), 250 (100%).

7-((5-(2-(Diethylamino)ethylthio)-4-(4-chlorophenyl)-4*H*-1,2,4-triazol-3-yl)methoxy)-3,4-dimethyl-2*H*-chromen-2-one (8b). Yield 74%; mp 118−120 °C; mol wt 513.05. IR (cm^{-1}, KBr): 3095 (CH aromatic stretching), 2968, 2931 (CH aliphatic stretching), 1702 (C═O, α-pyrone). ^{1}H NMR (DMSO-d_6, δ, ppm): 1.03 (6H, t, 2 $\underline{CH_3}CH_2$), 2.08 (3H, s, CH_3), 2.33 (3H, s, CH_3), 2.43 (4H, q, 2 $\underline{CH_2}CH_3$), 2.45 (2H, t, CH_2N), 3.26 (2H, t, CH_2S), 5.23 (2H, s, OCH_2), 6.81−7.62 (7H, m, Ar−H). MS *m*/*z* (RA %): 515 (M^+ + 2) (0.13%), 513 (M^+) (0.39%), 190 (7%), 99 (100%), 86 (66%).

7-((5-(2-Morpholinoethylthio)-4-(4-chlorophenyl)-4*H*-1,2,4-triazol-3-yl)methoxy)-4-methyl-2*H*-chromen-2-one (8c). Yield 80%; mp 86−89 °C; mol wt 513.01. IR (cm^{-1}, KBr): 3090 (CH aromatic stretching), 2945, 2850 (CH aliphatic stretching), 1733 (C═O, α-pyrone). ^{1}H NMR (DMSO-d_6, δ, ppm): 2.34 (3H, s, CH_3), 2.50 (4H, t, 2CH_2 N morpholine), 2.76 (2H, t, CH_2N), 3.46 (2H, t, CH_2S), 3.67 (4H, t, 2CH_2O morpholine), 5.08 (2H, s, OCH_2), 6.21 (1H, s, H-3 coumarin), 6.77−7.50 (7H, m, Ar−H). MS *m*/*z* (RA %): 515 (M^+ + 2) (0.03%), 513 (M^+) (0.1%), 176 (4%), 150 (10%), 114 (35%), 113 (100%).

7-((5-(2-Morpholinoethylthio)-4-(4-chlorophenyl)-4*H*-1,2,4-triazol-3-yl)methoxy)-3,4-dimethyl-2*H*-chromen-2-one (8d). Yield 81%; mp 174−6 °C; mol wt 527.03. IR (cm^{-1}, KBr): 3094 (CH aromatic stretching), 2936, 2863 (CH aliphatic stretching), 1698 (C═O, α-pyrone). ^{1}H NMR (DMSO-d_6, δ, ppm): 2.17 (3H, s, CH_3), 2.35 (3H, s, CH_3), 2.49 (4H, t, 2CH_2 N morpholine), 2.76 (2H, t, CH_2N), 3.46 (2H, t, CH_2S), 3.67 (4H, t, 2CH_2O morpholine), 5.08 (2H, s, OCH_2), 6.78−7.49 (7H, m, Ar−H). MS *m*/*z* (RA %): 529 (M^+ + 2) (0.03%), 527 (M^+) (0.1%), 190 (5%), 162 (2%), 114 (19%), 113 (100%).

General Procedure for Preparation of Schiff's Bases (9a−d). Schiff's bases (**9a**),[28] (**9b**), (**9c**),[28] and (**9d**) were prepared according to the reported method.[28]

2-(3,4-Dimethyl-2-oxo-2*H*-chromen-7-yloxy)-*N*′-(4-chlorobenzylidene)acetohydrazide (9b). Yield 80%; mp 233−5 °C; mol wt 384.81. Crystallization: AcOH. IR(cm^{-1}, KBr): 3211 (NH),3089 (CH aromatic stretching), 2964, 2854 (CH aliphatic stretching), 1719 (C═O, α-pyrone),1686 (C═O), 1626 (C═N). ^{1}H NMR (DMSO-d_6, δ, ppm): 2.04 (3H, s, CH_3), 2.34 (3H, s, CH_3), 5.25 (2H, s, OCH_2), 6.92−7.99 (7H, m, Ar−H), 8.00 (1H, s, CH═N), 11.7 (1H, s, NH, D_2O exchangeable). MS *m*/*z* (RA %): 386 (M^+ + 2) (3%), 384 (M^+) (10%), 283 (47%), 235 (100%), 219 (53%), 217(50%).

2-(3,4-Dimethyl-2-oxo-2*H*-chromen-7-yloxy)-*N*′-(1-(4-chlorophenyl)ethylidene)acetohydrazide (9d). Yield 78%; mp 228−230 °C; mol wt 398.84. Crystallization: AcOH. IR (cm^{-1}, KBr): 3084 (CH aromatic stretching), 2927 (CH aliphatic stretching), 1707 (C═O, α-pyrone), 1628 (C═O), 1611 (C═O). ^{1}H NMR (DMSO-d_6, δ, ppm): 2.04 (3H, s, CH_3), 2.25 (3H, s, CH_3), 2.33 (3H, s, CH_3), 5.28 (2H, s, OCH_2), 6.89−7.83 (7H, m, Ar−H), 10.95 (1H, s, NH, D_2O exchangeable). MS *m*/*z* (RA %): 400 (M^+ + 2) (12%), 398 (M^+) (32%), 211 (34%), 209 (100%), 188 (14%), 163(16%).

General Procedure for Preparation of 2-(4-Methyl (and/or 3,4-Dimethyl)coumarinyl-7-yloxy)-*N*-(2-(4-chlorophenyl)-4-oxothiazolidin-3-yl)acetamide (10a,b). A homogeneous mixture of the Schiff's bases (**9a,b**) (0.01 mol) and thioglycolic acid (0.92 g, 0.01 mol) in 20 mL of glacial acetic acid was refluxed for about 10 h. The reaction mixture was triturated with sodium bicarbonate (10%) solution, and the resulting neutral solution was poured onto crushed ice .The separated product was filtered off, washed with water, dried, and recrystallized from ethanol.

2-(4-Methyl-2-oxo-2*H*-chromen-7-yloxy)-*N*-(2-(4-chlorophenyl)-4-oxothiazolidin-3-yl)acetamide (10a). Yield 73%; mp 235−7 °C; mol wt 444.89. IR (cm^{-1}, KBr): 3130 (NH), 3001 (CH aromatic stretching), 2922, 2853(CH aliphatic stretching), 1722 (C═O, α-pyrone), 1615 (C═O). ^{1}H NMR (DMSO-d_6, δ, ppm): 2.31 (3H, s, CH_3), 3.74, 3.87 (2H, dd, CH_2 thiazolidinone), 4.79 (2H, s, OCH_2), 5.77 (1H, s, CH thiazolidinone), 6.17 (1H, s, H-3 coumarin), 6.74−7.60 (7H, m, Ar−H), 10.50 (1H, s, NH, D_2O exchangeable). MS *m*/*z* (RA %): 446 (M^+ + 2) (3%), 444 (M^+) (8%), 386 (25%), 312 (21%), 233 (100%), 212 (63%).

2-(3,4-Dimethyl-2-oxo-2*H*-chromen-7-yloxy)-*N*-(2-(4-chlorophenyl)-4-oxothiazolidin-3-yl)acetamide (10b). Yield 71%; mp 148−150 °C; mol wt 458.91. IR (cm^{-1}, KBr): 3237 (NH), 3001 (CH aromatic stretching), 2991, 2914(CH aliphatic stretching), 1693 (C═O, α-pyrone), 1612 (C═O). ^{1}H NMR (DMSO-d_6, δ, ppm): 2.04 (3H, s, CH_3), 2.32 (3H, s, CH_3), 3.74, 3.89 (2H, dd,CH_2

dx.doi.org/10.1021/jm301014y | J. Med. Chem. 2012, 55, 10424−10436

thiazolidinone), 4.79 (2H, s, OCH_2), 5.75 (1H, s, CH thiazolidinone), 6.75−7.60 (7H, m, Ar−H), 10.49 (1H, s, NH, D_2O exchangeable). MS *m*/*z* (RA %): 460 (M^+ + 2) (11%), 458 (M^+) (27%), 248 (9%), 247 (100%), 190 (32%), 189 (29%).

BIOLOGY

In Vitro Monoamine Oxidase A and B Inhibition. *Mitochondria Preparation.* Mitochondria were prepared according to Basford.[31] Reagents: medium A contained 0.4 M sucrose, 0.001 EDTA, 0.02% polyethersulfone (PES), or heparin, and pH was adjusted to 6.8−7.0 with KOH; medium F was made up of the medium A to which Ficoll was added to a final concentration of 8%.

Calf or beef brains were removed from the animals within 5−10 min after their death. The brains were immediately placed in cold medium A, stored on ice, and then transported to the laboratory. In a cold room, at 5 °C, the cerebral hemispheres were removed from the brains and the meninges were taken up with forceps. The gray matter was scraped from the cortices using a dull spatula. Two brains' yield corresponded to about 100 g of wet tissue, which was homogenized in medium A (2 mL/g of wet tissue). The homogenate was kept at pH 7.0 by adding some drops of Tris-buffer 2 M; 1 mg of ε-aminocaproic acid/g of tissue was added, and then the mixture was stirred at 0−4 °C for 15 min. The suspension was diluted with medium A (20 mL/g of the original tissue), centrifuged first at 184*g* for 20 min and then at 1153*g* for 20 min, without transferring of the supernatant. The residue R1 was discarded while the supernatant S1 was centrifuged at 12000*g* for 15 min to yield a crude mitochondria pellet R2 (the supernatant S2 which is discarded). The fraction R2 was suspended in medium F (6 mL/g of original tissue), gently homogenized, and centrifuged at 12000*g* for additional 30 min. The resulting mitochondria fraction R3 was washed using 4 mL of medium A/g of original tissue and again centrifuged at 12000*g* for 15 min. The final mitochondria fraction R4 was homogenized in potassium phosphate buffer pH 7.4, 0.25 M. The yield of mitochondria protein obtained was between 100 and 140 mg per 50 g wet weight of the original tissue.

Activity Assay. Monoamine oxidase activity was determined using kinuramine as a substrate, at four different final concentrations, ranging from 5 μM to 0.1 mM, by a sensitive fluorometric assay according to Matsumoto et al.[32] In all the assays, the incubation mixtures contained potassium phosphate buffer, pH 7.4, mitochondria (6 mg/mL), and drug solutions in DMSO and were added to the reaction mixture at a final concentration ranging from 0 to 10^{-9}.

Solutions were preincubated for 30 min before adding the substrate and then incubated for others 30 min. The inhibitory activities against MAO-A and MAO-B were determined at 38°C, after incubation of the mitochondrial fractions for 30 min in the presence of the specific inhibitor (L-deprenyl (1 μM) or clorgyline (1 μM) to estimate the MAO-A and MAOB activity, respectively). The addition of percloric acid ended the reaction. Then the samples were centrifuged at 10000g for 5 min and the supernatant was added to 2.7 mL of 1N NaOH. Fluorometric measurements were recorded at $\lambda_{exc.}$317 nm and λ_{em} 393 nm using a Perkin-Elmer LS 50B spectrofluorometer. Dixon plot were used to estimate the inhibition constant (K_i) of the inhibitors. Data are the means of three or more experiments each performed in duplicate.

In Vivo Tryptamine Seizure Potentiation in Rats. Groups of five male Wistar rats weighing 150−200 g were used. Test compounds, standard or vehicle controls, were administered intraperitoneally 0.5, 1, 2, and 4 h prior testing. At the time of testing, 5 mg/kg tryptamine HCl freshly dissolved in saline was injected intravenously. Immediately after tryptamine HCl administration, the animals were observed individually for three minutes for the appearance of clonic "pedalling" movements of the forepaws which is considered a positive response. Frequently, these clonic seizures were preceded by a kyphotic curvature of the spine, but this sign did not constitute a positive response. In addition to the vehicle control group, a series of five positive control animals receiving tranylcypromine at 5 mg/kg ip with a 30 min pretreatment time was subjected to the test in order to check the effectiveness of the tryptamine HCl solution which is relatively unstable. A 100% response was expected. Fresh tryptamine hydrochloride solution should be prepared hourly as needed. An ED_{50} was calculated using probitanalysis.[33,34]

Molecular Docking. The crystal structures of human MAO-A in complex with ligand **1** (PDB 2Z5X)[25] and the human MAO-B in complex with ligand **2** (PDB 2XFN)[39] were used for all simulations with the Autodock 4.2 suite.[38] All other docking conditions were as previously published.[41] The constructed 3D structures were energetically minimized by using MOPAC. AutoDock tool automatically computes Gasteiger charges and determines rotatable bonds of the ligand to be able to generate different conformers for the docking.

The grid maps of 60 × 60 × 60 grid points, centered on the ligands of the complex structures, were used to cover the binding pockets. A spacing of 0.375 Å was set centered at 41.126, 26.795, and −15.023 Å, respectively for MAO-A, that encompassed the active site where the cocrystallized ligand **1** was embedded, to be used to guide the docked inhibitors within MAO-A receptor, and flexible residues: Asn181, Phe208, Leu337 and Tyr444, whereas, The ligand **2** was centered into its MAO-B receptor at 50.655, 160.186, and 30.957 Å, respectively, and flexible residues Pro102, Ile199, Ile316, and Tyr326 were selected as key amino acids.

The Lamarckian genetic algorithm was used for all molecular docking simulations. Population size of 300, mutation rate of 0.02, and crossover rate of 0.8 were set as the parameters. Simulations were performed using up to 2.5 million energy evaluations with a maximum of 27000 generations. Each simulation was performed 10 times, yielding 10 docked conformations.

As a result of AutoDock calculations we obtained the output file with in our case 10 conformers of the protein−ligand complex with flexible residues. Each structure was scored and ranked by the program by its calculated interaction energies and similarities. The similarity of docked structures was measured by computing the root-mean-square deviation, RMSD, between the coordinates of the atoms.

ASSOCIATED CONTENT

Supporting Information

Elemental analysis and molecular docking details. This material is available free of charge via the Internet at http://pubs.acs.org.

AUTHOR INFORMATION

Corresponding Author

*Phone: +20 202 37608284. Fax: +20 202 33370931. E-mail: ommryan@yahoo.com.

Notes

The authors declare no competing financial interest.

■ ABBREVIATIONS USED

FAD, flavin adenine dinucleotide; K_i, inhibition constant; V_{max}, maximum velocity; K_m, Michaelis constant; PDB, Protein Data Bank; ED_{50}, median effective dose; DMSO, dimethylsulfoxide; TLC, thin layer chromatography; MOPAC, Molecular Orbital PACkage

■ REFERENCES

(1) Shih, J. C.; Chen, K.; Ridd, M. J. Monoamine oxidase: from genes to behavior. *Annu. Rev. Neurosci.* **1999**, *22*, 197−217.

(2) Shih, J. C.; Thompson, R. F. Monoamine oxidase in neuropsychiatry and behavior. *Am. J. Hum. Genet.* **1999**, *65*, 593−598.

(3) Chiba, K.; Trevor, A.; Castagnoli, N. Metabolism of the neurotoxic tertiary amine, MPTP, by brain monoamine oxidase. *Biochem. Biophys. Res. Commun.* **1984**, *120*, 574−578.

(4) Fritz, R. R.; Abell, C. W.; Patel, N. T.; Gessner, W.; Brossi, A. Metabolism of the neurotoxin in MPTP by human liver monoamine oxidase B. *FEBS Lett.* **1985**, *186*, 224−228.

(5) Grimsby, J.; Toth, M.; Chen, K.; Kumazawa, T.; Klaidman, L.; Adams, J. D.; Karoum, F.; Gal, J.; Shih, J. C. Increased stress response and beta-phenylethylamine in MAO-B-deficient mice. *Nature Genet.* **1997**, *17*, 206−210.

(6) Bach, A. W. J.; Lan, N. C.; Johnson, D. L.; Abell, C. W.; Bembenek, M. E.; Kwan, S. W.; Seeburg, P. H.; Shih, J. C. c DNA cloning of human liver monoamine oxidase A and B: molecular basis of differences in enzymatic properties. *Proc. Natl. Acad. Sci.U. S. A.* **1988**, *85*, 4934−4938.

(7) Johnston, J. P. Some observations upon a new inhibitor of monoamine oxidase in brain tissue. *Biochem. Pharmacol.* **1968**, *17*, 1285−1297.

(8) Kalgutkar, A. S.; Castagnoli, N., Jr.; Testa, B. Selective inhibitors of monoamine oxidase (MAO-A and MAO-B) as probes of its catalytic site and mechanism. *Med. Res. Rev.* **1995**, *15*, 325−388.

(9) Westlund, R. N.; Denney, R. M.; Kochersperger, L. M.; Rose, R. M.; Abell, C. W. Distinct monoamine oxidase A and B populations in primate brain. *Science* **1985**, *230*, 181−183.

(10) Knoll, J.; Magyar, K. Some puzzling pharmacological effects of monoamine oxidase inhibitors. *Adv. Biochem. Psychopharmacol.* **1972**, *5*, 393−408.

(11) Rudorfer, M. V.; Potter, V. Z. Antidepressants. A comparative review of the clinical pharmacology and therapeutic use of the "newer" versus the "older" drugs. *Drugs* **1989**, *37*, 713−738.

(12) Gerlach, M.; Double, K.; Reichmann, H.; Riederer, P. Arguments for the use of dopamine receptor agonists in clinical and preclinical Parkinson's diseases. *J. Neural. Transm. Suppl.* **2003**, *65*, 167−83.

(13) Riederer, P.; Danielczyk, W.; Grunblatt, E. Monoamine oxidase-B inhibition in Alzheimer's disease. *Neurotoxicology* **2004**, *25*, 271−277.

(14) Matos, M. J.; Terán, C.; Castillo, Y. P.; Uriarte, E.; Santana, L.; Viña, D. Synthesis and Study of a Series of 3-Arylcoumarins as Potent and Selective Monoamine Oxidase B Inhibitors. *J. Med. Chem.* **2011**, *54*, 7127−7137.

(15) Chimenti, F.; Secci, D.; Bolasco, A.; Chimenti, P.; Granese, A.; Befani, O.; Turini, P.; Alcaroc, S.; Ortuso, F. Inhibition of monoamine oxidases by coumarin-3-acyl derivatives: biological activity and computational study. *Bioorg. Med. Chem. Lett.* **2004**, *14*, 3697−3703.

(16) Secci, D.; Carradori, S.; Bolasco, A.; Chimenti, P.; Yáñez, M.; Ortuso, F.; Alcaro, S. Synthesis and selective human monoamine oxidase inhibition of 3-carbonyl, 3-acyl, and 3-carboxyhydrazido coumarin derivatives. *Eur. J. Med. Chem.* **2011**, *46*, 4846−4852.

(17) Gnerre, C.; Catto, M.; Leonetti, F.; Weber, P.; Carrupt, P. A.; Altomare, C.; Carotti, A.; Testa, B. Inhibition of Monoamine Oxidases by Functionalized Coumarin Derivatives: Biological Activities, QSARs, and 3D-QSARs. *J. Med. Chem* . **2000**, *43*, 4747−4758.

(18) Carotti, A.; Altomare, C.; Catto, M.; Gnerre, C.; Summo, L.; De Marco, A.; Rose, S.; Jenner, P.; Testa, B. Lipophilicity plays a major role in modulating the inhibition of monoamine oxidase B by 7-substituted coumarins. *Chem. Biodiversity* **2006**, *3*, 134−149.

(19) Maccioni, E.; Alcaro, S.; Cirilli, R.; Vigo, S.; Cardia, M. C; Sanna, M. L.; Meleddu, R.; Yanez, M.; Costa, G.; Casu, L.; Matyus, P.; Distinto, S. 3-Acetyl-2,5-diaryl-2,3-dihydro-1,3,4-oxadiazoles: a new scaffold for the selective inhibition of monoamine oxidase B. *J. Med. Chem.* **2011**, *54*, 6394−6398.

(20) Mazouz, F.; Gueddari, S.; Burstein, C.; Mansuy, D.; Milcent, R. 5-[4-(Benzyloxy) phenyl]-1,3,4-oxadiazol-2(3*H*)-one derivatives and related analogues: new reversible, highly potent, and selective monamine oxidase type B inhibitors. *J. Med .Chem.* **1993**, *36*, 1157−1167.

(21) Drescher, K.; Fischer von Weikersthal, S.; Weifenbach, H.; Traut, M. Characterization of the selective and reversible monoamine oxidase B inhibitor LU 53439 in vitro and in vivo. *Naunyn-Schmiedeberg's Arch. Pharmacol.* **1993**, *347* (Suppl), R135.

(22) Frickel, F. F.; Kuekenhoehner, T.; Rendenbach-Mueller, B.; Weifenbach, H.; Teschendorf, H. J. Alkoxycoumarins substituted by a heterocyclic radical, their preparation and therapeutic agents containing these compounds. US Patent 5,073,563, 1991.

(23) Husain, M. I.; Amir, M.; Singh, E. Synthesis of some new substituted mercaptotriazoles and thiazolidones and their monoamine oxidase inhibitory and anticonvulsant properties. *Indian J. Chem., Sect. B* **1987**, *26*, 251−254.

(24) Hubálek, F.; Binda, C.; Khalil, A.; Li, M.; Mattevi, A.; Castaganoli, N.; Edmondson, D. E. Demonstration of isoleucine 199 as a structural determinant for the selective inhibition of human monoamine oxidase B by specific reversible inhibitors. *J. Biol. Chem.* **2005**, *280*, 15761−15766.

(25) Son, S.-Y.; Ma, J.; Kondou, Y.; Yoshimura, M.; Yamashita, E.; Tsukihara, T. Stucture of human monoamine oxidase A at 2.2 Å resolution: the control of opening the entry for substrates/inhibitors. *Proc. Natl. Acad. Sci. U. S. A.* **2008**, *105*, 5739−5744.

(26) Binda, C.; Wang, J.; Pisani, L.; Caccia, C.; Carotti, A.; Salvati, P.; Edmondson, D. E.; Mattevi, A. Structures of human monoamine oxidase B complexes with selective noncovalent inhibitors: safinamide and coumarin analogs. *J. Med. Chem.* **2007**, *50*, 5848−5852.

(27) Eid, A. I.; Ragab, F. A.; El-Ansary, S. L.; El-Gazayerly, S. M.; Mourad, F. E. Synthesis of new 7-substituted 4-methylcoumarin derivatives of antimicrobial activity. *Arch. Pharm. (Weinheim)* **1994**, *327*, 211−213.

(28) Imtiaz Husain, M.; Shukla, M. K.; Agarwal, S. K. Search for potent anthelimentics, Part VII. Hydrazones derived from 4-substituted-7-coumarinyloxyacetic acid hydrazide. *J. Indian Chem. Soc.* **1979**, *56*, 306−307.

(29) Karl, U.; Rendenbach-Mueller, B. Preparation of substituted thiadiazolyl-methoxycoumarins. *Ger.Offen.* 1996, DE 4435250 A1 19960411.

(30) Bhavsar, S. B.; Shinde, D. B. Synthesis of substituted coumarinyl-oxytriazoles and thiadiazoles and their antimicrobial activity. *Ind. J. Chem, Sect. B.* **1995**, *34*, 70−74.

(31) Basford, R. E. Preparation and properties of brain mitochondria. *Methods Enzymol.* **1967**, *10*, 96−101.

(32) Matsumoto, T.; Suzuki, O.; Furuta, T.; Asai, M.; Kurokawa, Y.; Rimura, Y.; Katsumata, Y.; Takahashi, I. A sensitive fluorometric assay for serum monoamine oxidase with kynuramine as substrate. *Clin. Biochem.* **1985**, *18*, 126−129.

(33) Knoll, J. Monoamine oxidase inhibitors: Chemistry and pharmacology. In: *Enzyme Inhibitors as Drugs*; Sandler, M., Ed.; University Park Press: Baltimore, MD, 1980; pp 151−173.

(34) Ozaki, M.; Weissbach, H.; Ozaki, A.; Witkop, B.; Udenfriend, S. Monoamine oxidase inhibitors and procedures for their evaluation in vivo and in vitro. *J. Med. Pharm. Chem.* **1960**, *2*, 591−607.

(35) Binda, C.; Newton-Vinson, P.; Hubalek, F.; Edmondson, D. E.; Mattevi, A. Structure of human monoamine oxidase B, a drug target for the treatment of neurological disorders. *Nature Struct. Biol.* **2002**, *9*, 22−26.

(36) Ma, J. C.; Yoshimura, M.; Yamashita, E.; Nakagawa, A.; Ito, A.; Tsukihara, T. Structure of rat monoamine oxidase A and its specific recognitions for substrates and inhibitors. *J. Mol. Biol.* **2004**, *338*, 103−114.
(37) Binda, C.; Li, M.; Hubalek, F.; Restelli, N.; Edmondson, D. E.; Mattevi, A. Insights into the mode of inhibition of human mitochondrial monoamine oxidase B from high-resolution crystal structures. *Proc. Natl. Acad. Sci. U. S. A.* **2003**, *100*, 9750−9755.
(38) Morris, G. M.; Huey, R.; Lindstrom, W.; Sanner, M. F.; Belew, R. K.; Goodsell, D. S.; Olson, A. J. AutoDock 4 and AutoDock Tools 4: Automated Docking with Selective Receptor Flexibility. *J. Comput. Chem.* **2009**, *30*, 2785−2791.
(39) Bonivento, D.; Milczek, E. M.; McDonald, G. R.; Binda, C.; Holt, A.; Edmondson, D. E.; Mattevi, A. Potentiation of ligand binding through cooperative effects in monoamine oxidase B. *J. Biol. Chem.* **2010**, *285*, 36849−36856.
(40) Wang, R.; Wang, Y.; Lu, S. Comparative evaluation of 11 scoring functions for molecular docking. *J. Med. Chem.* **2003**, *46*, 2287−2303.
(41) Abdelhafez, O. M.; Amin, K. M.; Ali, H. I.; Maher, T. J.; Batran, R. Z. Dopamine release and molecular modeling study of some coumarin derivatives. *Neurochem. Int.* **2011**, *59*, 906−912.